Applied and Environmental Microbiology

Monitoring the Metabolic State of Fungal Hyphae and the Presence of Melanin by Nonlinear Spectral Imaging

Helene Knaus, Gerhard A. Blab, Alexandra V. Agronskaia, Dave J. van den Heuvel, Hans C. Gerritsen and Han A. B. Wösten

Appl. Environ. Microbiol. **2013, 79(20):6345. DOI: 10.1128/AEM.02291-13.**
Published Ahead of Print 9 August 2013.

AEM
Journals.ASM.org

Monitoring the Metabolic State of Fungal Hyphae and the Presence of Melanin by Nonlinear Spectral Imaging

Helene Knaus,[a,b] Gerhard A. Blab,[b] Alexandra V. Agronskaia,[b] Dave J. van den Heuvel,[b] Hans C. Gerritsen,[b] Han A. B. Wösten[a]

Microbiology and Kluyver Centre for Genomics of Industrial Fermentation, Utrecht University, Utrecht, The Netherlands[a]; Molecular Biophysics, Debye Institute, Utrecht University, Utrecht, The Netherlands[b]

Label-free nonlinear spectral imaging microscopy (NLSM) records two-photon-excited fluorescence emission spectra of endogenous fluorophores within the specimen. Here, NLSM is introduced as a novel, minimally invasive method to analyze the metabolic state of fungal hyphae by monitoring the autofluorescence of NAD(P)H and flavin adenine dinucleotide (FAD). Moreover, the presence of melanin was analyzed by NLSM. NAD(P)H, FAD, and melanin were used as biomarkers for freshness of mushrooms of *Agaricus bisporus* (white button mushroom) that had been stored at 4°C for 0 to 17 days. During this period, the mushrooms did not show changes in morphology or color detectable by eye. In contrast, FAD/NAD(P)H and melanin/NAD(P)H ratios increased over time. For instance, these ratios increased from 0.92 to 2.02 and from 0.76 to 1.53, respectively, at the surface of mushroom caps that had been harvested by cutting the stem. These ratios were lower under the skin than at the surface of fresh mushrooms (0.78 versus 0.92 and 0.41 versus 0.76, respectively), indicative of higher metabolism and lower pigment formation within the fruiting body. Signals were different not only between tissues of the mushroom but also between neighboring hyphae. These data show that NLSM can be used to determine the freshness of mushrooms and to monitor the postharvest browning process at an early stage. Moreover, these data demonstrate the potential of NLSM to address a broad range of fundamental and applied microbiological processes.

Worldwide, the annual production of edible mushrooms amounts to approximately 7.7 million tons. The white button mushroom, *Agaricus bisporus*, is one of the most important commercial species. It is low in fat and rich in fiber, vitamins, minerals, linoleic acid, and bioactive compounds such as anticancer polysaccharides (1–3). Moreover, the button mushroom contains more digestible proteins than most vegetables and only slightly less than meat products and milk (4, 5). Mushrooms are a perishable product. Therefore, there is a need for tools to monitor freshness of fruiting bodies. These tools could also be applied in breeding programs and to improve storage conditions.

The metabolic state and melanin formation could be used as indicators for freshness of mushrooms. The presence of melanin can be detected by various microscopic techniques (6–8). There are also several methods to quantify the metabolic activity of fungi. They are often based on fluorescence assays monitoring the activity of NADH-dependent dehydrogenases (9) or NADH-dependent oxidoreductases (10, 11) or by viability stains that are metabolized in the presence of ATP and intracellular esterases (12). Most of these assays require cell extracts, tissue sectioning, and incorporation of marker molecules into cells. Nonlinear spectral microscopy (NLSM) is a potent, noninvasive (13–17) alternative to monitor the metabolic state and the presence of melanin in fungi. NLSM maps (auto)fluorescence emission spectra within the specimen (18–20). Phototoxicity of this technique is low because excitation is limited to the focal volume. The recorded emission spectrum of a specimen is a combination of the spectra of the individual fluorophores. NAD(P)H, flavin adenine dinucleotide (FAD), and melanin are autofluorescent molecules that occur in fungi (21). These compounds have maximum emission in the blue (460-nm), green (530-nm), and red (620-nm) wavelength ranges, respectively (18, 22). Quantification of the contribution of each fluorophore is possible by decomposition of the measured emission spectrum. Such unmixing methods rely mostly on reference spectra or presumptions of the components (23, 24), but recently, "blind unmixing," not requiring *a priori* knowledge of the autofluorescent components, has been introduced (25).

We show here that NLSM can be used to monitor freshness of *Agaricus bisporus* mushrooms using NAD(P)H, FAD, and melanin as biomarkers. These results illustrate that NLSM has potential use in fundamental and applied microbiological research, for instance, in monitoring fungal activity in bioreactors.

MATERIALS AND METHODS

Growth and storage of *A. bisporus*. Plastic containers (17.5 by 27.5 by 22.5 cm) were filled with 3.5 kg phase III compost colonized with *A. bisporus* strain Sylvan A15 (CNC Grondstoffen, Milsbeek, The Netherlands) and topped with 1 kg of casing soil (CNC Grondstoffen). The cultures were incubated at 24°C and 95% relative humidity (RH) in Economic Premium Climate chambers (Snijders Scientific, Tilburg, The Netherlands). Water (200 ml) was added to each of the containers during the first 4 days of incubation. Growth was prolonged at 20°C and 88% RH when aggregates had formed on the casing layer (i.e., after 14 days of culturing). Mushroom caps with a diameter of about 5.5 cm were selected for NLSM. Mushrooms were harvested either by picking or by cutting the stem. They were stored in plastic bags at 4°C.

Nonlinear spectral imaging. A schematic diagram of the nonlinear spectral imaging setup is shown in Fig. 1. An Eclipse Ti-U inverted microscope (Nikon Instruments Europe, Amsterdam, The Netherlands) was used with a CFI S Fluor 20× air objective (numerical aperture [NA], 0.75; Nikon Instruments Europe). The excitation source was a tunable Chame-

Received 11 July 2013 Accepted 3 August 2013
Published ahead of print 9 August 2013
Address correspondence to Han A. B. Wösten, h.a.b.wosten@uu.nl.

doi:10.1128/AEM.02291-13

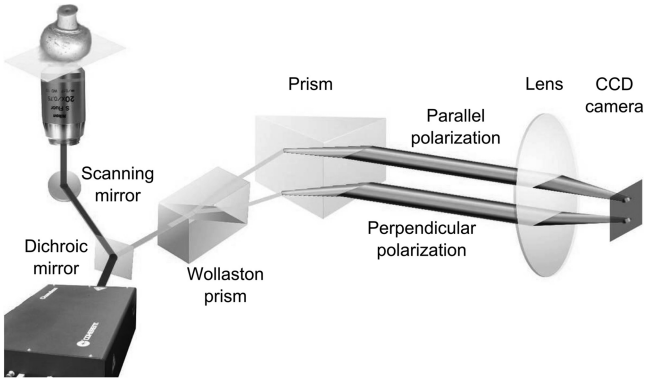

FIG 1 Schematic representation of the nonlinear spectral imaging setup.

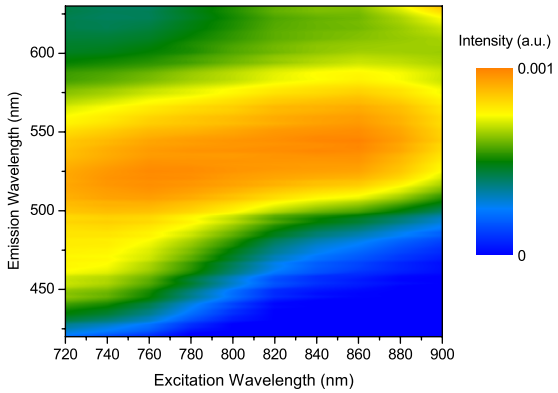

FIG 2 Excitation-emission matrix of a peeled cap of a freshly cut *A. bisporus* mushroom. The color map represents intensity. Data were measured in 20-nm bins and smoothed with OriginLab.

leon Ultra II mode-locked titanium-sapphire laser (Coherent Europe, Utrecht, The Netherlands). It was coupled directly to a C1 confocal scan head (Nikon Instruments Europe), in which the fiber coupling unit was removed. The emission was reflected by a T680dcspxr multiphoton dichroic mirror (Chroma Technology, Olching, Germany) within the scan head. The emission was guided via a high-reflectance MaxMirror (Semrock, Rochester, NY, USA) and an FF01-680/SP-25 BrightLine multiphoton short-pass emission filter (Semrock) through a periscope (containing two high-reflectance MaxMirrors) to the spectrograph. The spectrograph consisted of a quartz 0.5° Wollaston prism (MWQ25-05-HEAR, 450 to 750 nm; Karl Lambrecht, Chicago, IL, USA), a 056-0120 BK7 equilateral prism (OptoSigma, Santa Ana, CA, USA), a 026-0770 achromatic doublet lens (diameter of 25 mm, focal length of 119.8 mm, and broadband antireflection at 425 to 675 nm; OptoSigma), and an IxonEM 860 electron multiplication charge-coupled-device (CCD) camera (Andor, Belfast, United Kingdom).

The wavelength calibration of the spectrograph was carried out by measuring two-photon spectra of Lucifer Yellow (Life Technologies Europe, Bleiswijk, The Netherlands), 7-methoxycoumarin-4-acetic acid (Sigma-Aldrich Chemie, Zwijndrecht, The Netherlands), and coumarin 120 (Aldrich) with and without the following optical filters: the 390/482/563/640-nm BrightLine filter (Semrock); the 633-nm, 514-nm, and 442-nm RazorEdge (Semrock) filters; the HQ 585/40m and the HQ 510/50m (Chroma Technology) filters; and the Ex 450-490 and the BA 420 Nikon Fluorescence Filter Cube filters. The spectral response correction of the instrument was determined by using secondary emission standards, as described previously (26). As secondary emission standards, Lucifer Yellow and coumarin 120 were chosen.

Nonlinear spectral images (256 by 256 pixels; 400 by 400 μm) were acquired with an exposure time of 400 μs per pixel and a power of 14 mW at the specimen. Emission spectra were recorded for excitation wavelengths ranging from 720 nm to 940 nm (in 20-nm steps), while keeping the power at the specimen constant. All other images were recorded with an excitation wavelength of 765 nm. The storage experiment was performed in duplicate. Under each condition (cut and picked mushrooms, and peeled and unpeeled caps), five mushrooms were examined at five randomly chosen spots. For the heat treatment experiment, a freshly harvested mushroom was imaged before and after incubation in water at 65°C for 10 min.

Data analysis. All data were background subtracted before further analysis. For visualization purposes, the spectral images are represented in "real color." To this end, the spectral information of each pixel was transformed into red-blue-green (RGB) values that resemble the color of the fluorescence emission perceived by eye (27). Spectral decomposition was performed by using spectral phasor analysis (28), yielding the fractional intensities of NAD(P)H, FAD, and melanin. The reference signatures of FAD and NADH were obtained by acquiring two-photon-excited spectra of 2 mg ml^{-1} FAD (Sigma-Aldrich Chemie) in H_2O and 2.3 mM NADH (Sigma-Aldrich Chemie) in 100 mM 3-(*N*-morpholino)propanesulfonic acid (Sigma-Aldrich Chemie) buffer (pH 7.4), yielding emission peaks of 460 nm and 530 nm, respectively. The emission peak of melanin (620 nm) was taken from data reported previously (22). For every nonlinear spectral image, the fractional intensities of NAD(P)H, FAD, and melanin were used to calculate the average ratios of FAD/NAD(P)H and melanin/NAD(P)H. Error bars represent errors of the means of 50 measurements. Statistical analysis was performed by using OriginPro 8 SR2 (OriginLab, Northampton, MA, USA) using two-sample *t* tests (unequal variance) with a *P* value of ≤0.05.

RESULTS

Spectral characterization of the specimen. Emission spectra of a freshly cut mushroom were recorded between 425 nm and 650 nm using excitation wavelengths ranging from 720 nm to 940 nm. The skin of the cap was peeled to exclude an impact of autofluorescent molecules of bacteria residing on the mushroom surface. The resulting excitation-emission matrix (Fig. 2) shows that two-photon excitation should be between 720 and 780 nm to excite all endogenous fluorophores emitting between 425 and 650 nm [i.e., NAD(P)H, FAD, and melanin].

Monitoring the metabolic state and aging of fungal hyphae. Nonlinear spectral images of freshly cut mushroom caps of *A. bisporus* were recorded using an excitation wavelength of 765 nm (Fig. 3). The broad-emission spectrum (Fig. 3C) showed a high intensity between 450 and 500 nm, indicative of the presence of NAD(P)H. The spectrum was clearly red shifted when the mushroom had been incubated for 10 min at 65°C (Fig. 3C). Note that the spectra were recorded under the same imaging conditions. The shoulder peak in the blue spectral range, attributed mainly to the presence of NAD(P)H (18, 20), had disappeared. At the same time, the red part of the spectrum (>600 nm) had increased, which is likely due to the presence of melanin. Indeed, browning of the mushroom after the heat treatment was detectable even by eye. Thus, inactivation of *A. bisporus* hyphae by heat treatment was accompanied by a blue- to red-shifted spectrum.

In the next set of experiments, we examined whether a blue- to red-shifted spectrum can be also observed upon storage of *A. bisporus* mushrooms at 4°C. To this end, the surface of mushroom caps was imaged directly or after peeling off the skin tissue. The latter was done to exclude an impact of autofluorescent molecules of bacteria that reside at the surface of the cap. The mushrooms were harvested either by cutting the stipe (mimicking the harvest-

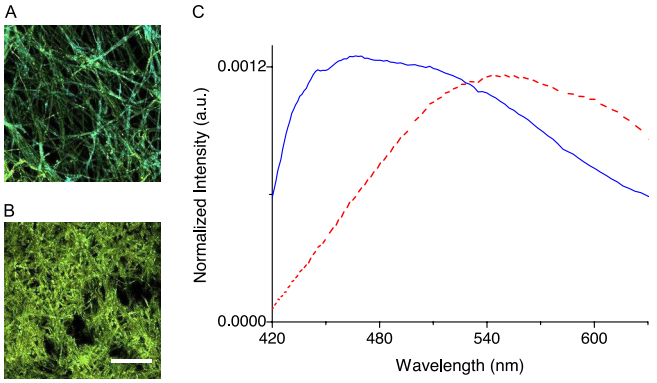

FIG 3 (A and B) Nonlinear spectral images of the cap of a freshly harvested *A. bisporus* mushroom before (A) and after (B) incubation for 10 min at 65°C. The color of each pixel in the images is the result of the relative contribution of RGB values to the total fluorescence intensity. (C) Average spectrum in panel A shown as a solid line and in panel B shown as a dashed line. The bar represents 100 μm. a.u., arbitrary units.

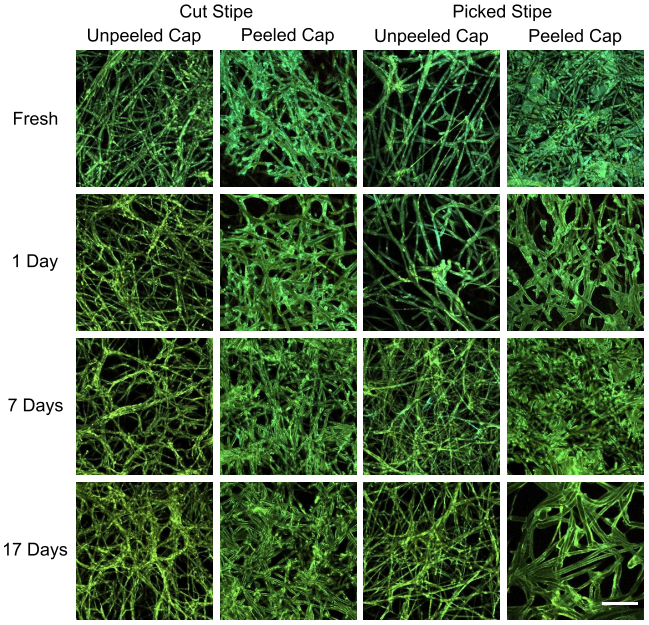

FIG 4 Nonlinear spectral images of *A. bisporus* caps showing the effect of storage at 4°C (excitation at 765 nm). The color of each pixel in the images is the result of the relative contribution of RGB values to the total fluorescence intensity. Mushroom caps were imaged after picking (picked stipe) or cutting of the stipe (cut stipe) and after removal (peeled) of the skin layer or not (unpeeled). Images represent freshly harvested mushrooms and mushrooms stored for 1, 7, and 17 days. The bar represents 100 μm.

ing process in commercial mushroom farming) or by gently picking them from the bed. In the latter case, casing soil and vegetative mycelium remained attached to the lower part of the stipe. In all cases, the morphology and color of the mushrooms did not change during the 17-day storage period, as detected by eye. Nonlinear spectral images of hyphae of unpeeled caps were more heterogeneous than those exposed after peeling of the skin (Fig. 4). Generally, fresh mushrooms exhibited a blue-green average spectrum (Fig. 4). This was most obvious for peeled mushroom caps. Mushrooms stored for 1 day already appeared greener in the RGB images (Fig. 4). This red shift was even more pronounced by extending the storage time. To quantify these spectral differences, the emission spectra were decomposed into the main components by spectral phasor analysis, resulting in the spectral contributions of NAD(P)H, FAD, and melanin (Fig. 5). With increasing storage times, the relative melanin and FAD contributions were increasing, while the NAD(P)H contribution was decreasing. The metabolic state expressed as the FAD/NAD(P)H ratio changed from 0.94 to 1.12 after 2 days of storage in the case of cut-stipe unpeeled mushrooms (Fig. 6A and data not shown). This ratio remained unchanged at between 2 and 7 days but had increased to 2.02 after 17 days of storage. Notably, the FAD/NAD(P)H ratio had increased already after 1 day from 0.78 to 1.05 in peeled cut-stipe caps. This ratio had further increased to 1.19 after 2 days of storage. No changes were detected at between 2 and 7 days of storage, but after 17 days, the FAD/NAD(P)H ratio had increased to 1.96 (Fig. 6C and data not shown). Unpeeled picked mushrooms showed a slight, if any, decrease in the FAD/NAD(P)H ratio between harvesting and 7 days of storage. Only after 17 days did the ratio increase from 0.89 to 1.59 (Fig. 6B and data not shown). This ratio is lower than that of cut-stipe mushrooms after 17 days (Fig. 6A). When the skin layer was removed, picked mushrooms followed the same trend as cut-stipe mushrooms. Similar to peeled cut-stipe caps, a significant increase in the FAD/NAD(P)H ratio from 0.73 to 0.91 was found after 1 day of storage. At between 1 and 7 days of storage at 4°C, no significant changes were detected. Only after 17 days of storage did the FAD/NAD(P)H ratio increase to 1.46 (Fig. 6D and data not shown).

Cut-stipe unpeeled mushrooms exhibited an increase in the melanin/NAD(P)H ratio from 0.76 to 0.88 after 2 days of storage. No changes were observed at between 2 and 7 days of storage, but the value had increased to 1.53 after 17 days of storage (Fig. 6A and data not shown). Significant differences in the melanin/NAD(P)H ratio were detected (from 0.41 to 0.50) after 1 day of storage when the skin layer was removed from the cap. Similar to unpeeled cut-stipe mushrooms, no differences were observed at between 2 and 7 days of storage, while after 17 days, the melanin/NAD(P)H ratio increased to 1.08 (Fig. 6C and data not shown). Unpeeled picked-stipe mushrooms showed no changes in the melanin/NAD(P)H ratio during the first 7 storage days, but the ratio had increased from 0.63 to 1.18 after 17 days of storage (Fig. 6C and D and data not shown). Freshly picked peeled mushrooms had a lower melanin/NAD(P)H ratio than those that had been stored. In addition, picked peeled mushrooms that had been stored for 17 days had a higher melanin/NAD(P)H ratio than the mushrooms stored for 1 to 7 days (Fig. 6D and data not shown).

DISCUSSION

This study combined NLSM with spectral phasor analysis as a novel, minimally invasive method to study the effect of storage on metabolism and pigment formation in *A. bisporus* mushrooms. To this end, the endogenous fluorophores NAD(P)H, FAD, and melanin were used as biomarkers directly at the surface of the mushroom and after removing the peel. Unpeeled caps showed in general a greater variation in their spectra than did peeled caps. This may be due to a higher variation in metabolism and melanin formation between hyphae that make up the surface layer of the mushroom. It may also be caused by bacteria that colonize the surface of the mushroom (29, 30). Nevertheless, changes in the spectra of unpeeled and peeled surfaces followed the same trend.

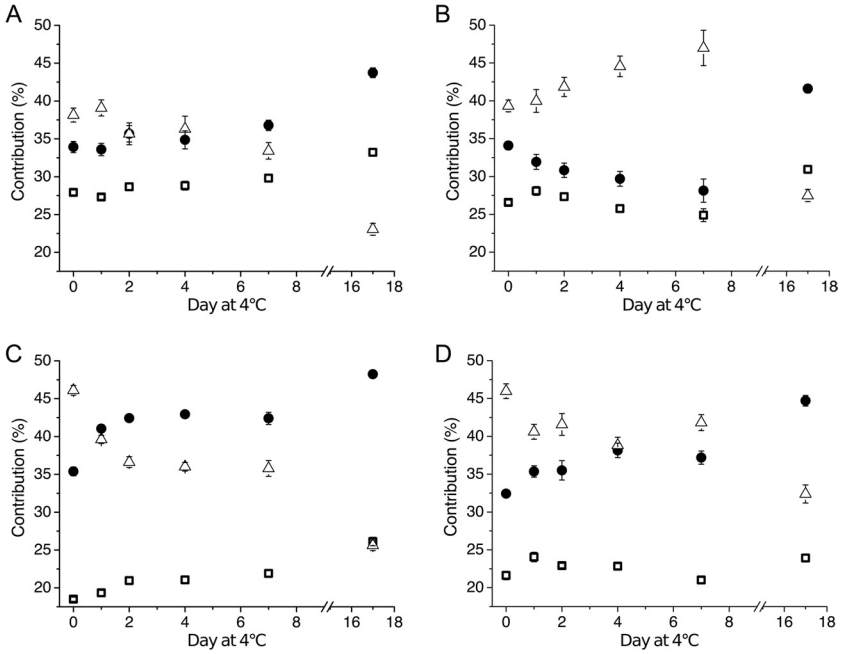

FIG 5 Contribution of NAD(P)H (triangles), FAD (circles), and melanin (squares) as a percentage of the emission spectrum of *A. bisporus* caps that had been stored for 0 to 17 days at 4°C. NLSM images were acquired for cut-stipe and unpeeled caps (A), picked-stipe and unpeeled caps (B), cut-stipe and peeled caps (C), and picked-stipe and peeled caps (D), using excitation at 765 nm. The contribution of the autofluorescent components was determined by using spectral decomposition.

Spectra of *A. bisporus* mushroom caps change upon storage at 4°C. The contribution of NAD(P)H to the total spectrum is decreasing while the contribution of FAD and melanin is increasing over time. NAD(P)H is oxidized in the electron transport chain to nonfluorescent NAD(P) for ATP production. Decreasing fluorescence emission of NAD(P)H indicates less or no new NAD(P)H formation within the glycolysis and the citric acid cycle. Nonfluorescent reduced flavin adenine dinucleotide ($FADH_2$) is also produced in the citric acid cycle and is also oxidized in the electron transport chain, yielding fluorescent FAD. Thus, none or little $FADH_2$ formation within the citric acid cycle coincides with increasing FAD emissions. The FAD/NAD(P)H ratio can therefore

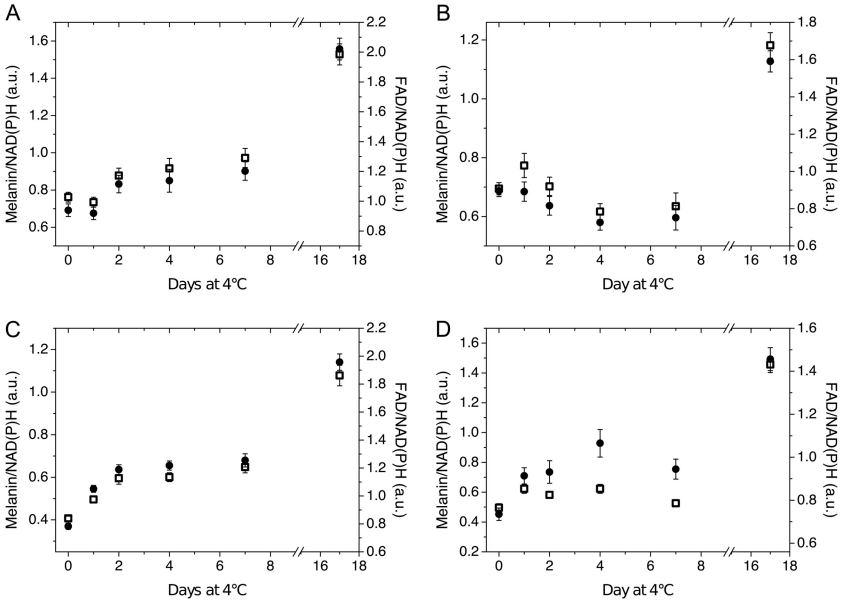

FIG 6 Changes in FAD/NAD(P)H (circles) and melanin/NAD(P)H (squares) ratios in the two-photon-excited emission spectra during storage of *A. bisporus* mushrooms at 4°C. NLSM images were acquired for cut-stipe and unpeeled caps (A), picked-stipe and unpeeled caps (B), cut-stipe and peeled caps (C), and picked-stipe and peeled caps (D), using excitation at 765 nm.

be considered an indicator of metabolic activity (31). This ratio increased upon storage of *A. bisporus* mushrooms, especially in the case of fruiting bodies that had been harvested by cutting. The vegetative mycelium and casing layer remain attached to the mushroom when fruiting bodies are harvested by picking. The vegetative mycelium may still have some feeding capacity, and at the same time, picking may prevent drying out of the fruiting body.

It is known that mechanical damage (32) or infection (33, 34) of mushrooms results in the formation of melanin. Normally, tyrosinase and its phenol substrates are spatially separated, but when brought together, melanin synthesis is initiated (35–37). The melanin contribution to the total spectrum increased during storage, while the NAD(P)H contribution decreased (Fig. 5). As a result, melanin/NAD(P)H ratios increased during storage. In general, cut-stipe mushrooms exhibited higher melanin/NAD(P)H ratios than picked-stipe caps. In fact, FAD/NAD(P)H and melanin/NAD(P)H ratios followed the same trend. This suggests that a reduction in metabolic activity is accompanied by melanin formation.

Freshly harvested mushrooms exhibited lower FAD/NAD(P)H and melanin/NAD(P)H ratios underneath the skin than on the surface layer. This can be explained by a higher metabolic activity of the hyphae under the peel and at the same time by reduced melanin formation in this tissue. These data thus show that zones within the mushroom are heterogeneous with respect to metabolism and pigment formation. Such zonal heterogeneity was also shown previously with respect to gene expression (38–44) and protein accumulation (39) in *A. bisporus*. In fact, these processes can be heterogeneous even between neighboring hyphae within a mycelial zone (45–49). Spectra of neighboring hyphae at the surface and under the peel of the mushroom were also heterogeneous (Fig. 4). These differences may be due partly to the bacterial load in the case of the skin but can be attributed only to the heterogeneity of metabolism and pigment formation under the peel.

To summarize, NLSM provides an excellent alternative to conventional methods that are used to monitor the metabolic activity of cells. It is noninvasive, shows reduced phototoxicity compared to other imaging methods, does not depend on exogenous molecules, and provides spectral and spatial information down to the subcellular level. We have shown that NLSM can be used to predict freshness of mushrooms by monitoring their metabolism. Monitoring metabolism is also of interest for bioprocess modeling, controlling fermentations in bioreactors, and cell biology studies of microbes.

ACKNOWLEDGMENTS

We thank H. H. Truong and F. Fereidouni for helpful discussions.

This work was supported by the Dutch Technology Foundation STW, the Applied Science Division of the NWO, and the Technology Program of the Ministry of Economic Affairs.

REFERENCES

1. **Mattila P, Könkö K, Eurola M, Pihlava J, Astola J, Vahteristo L, Hietaniemi V, Kumpulainen J, Valtonen M, Piironen V.** 2001. Contents of vitamins, mineral elements, and some phenolic compounds in cultivated mushrooms. J. Agric. Food Chem. **49:**2343–2348.
2. **Kozarski M, Klaus A, Niksic M, Jakovljevic D, Helsper JP, Van Griensven LJ.** 2011. Antioxidative and immunomodulating activities of polysaccharide extracts of the medicinal mushrooms *Agaricus bisporus*, *Agaricus brasiliensis*, *Ganoderma lucidum* and *Phellinus linteus*. Food Chem. **129:**1667–1675.
3. **Jeong SC, Jeong YT, Yang BK, Islam R, Koyyalamudi SR, Pang G, Cho KY, Song CH.** 2010. White button mushroom (*Agaricus bisporus*) lowers blood glucose and cholesterol levels in diabetic and hypercholesterolemic rats. Nutr. Res. **30:**49–56.
4. **Wani BA, Bodha R, Wani A.** 2010. Nutritional and medicinal importance of mushrooms. J. Med. Plant Res. **4:**2598–2604.
5. **Kurtzman RH, Jr.** 1997. Nutrition from mushrooms, understanding and reconciling available data. Mycoscience **38:**247–253.
6. **Butler M, Gardiner R, Day A.** 2005. Fungal melanin detection by the use of copper sulfide-silver. Mycologia **97:**312–319.
7. **Eisenman HC, Nosanchuk JD, Webber JBW, Emerson RJ, Camesano TA, Casadevall A.** 2005. Microstructure of cell wall-associated melanin in the human pathogenic fungus *Cryptococcus neoformans*. Biochemistry **44:**3683–3693.
8. **Hegnauer H, Nyhle'n LE, Rast DM.** 1985. Ultrastructure of native and synthetic *Agaricus bisporus* melanins—implications as to the compartmentation of melanogenesis in fungi. Exp. Mycol. **9:**1–29.
9. **Harris DM, Diderich JA, Van der Krogt ZA, Luttik MAH, Raamsdonk LM, Bovenberg RAL, Van Gulik WM, Van Dijken JP, Pronk JT.** 2006. Enzymic analysis of NADPH metabolism in β-lactam-producing *Penicillium chrysogenum*: presence of a mitochondrial NADPH dehydrogenase. Metab. Eng. **8:**91–101.
10. **Moss BJ, Kim Y, Nandakumar M, Marten MR.** 2008. Quantifying metabolic activity of filamentous fungi using a colorimetric XTT assay. Biotechnol. Prog. **24:**780–783.
11. **Kuhn D, Balkis M, Chandra J, Mukherjee P, Ghannoum M.** 2003. Uses and limitations of the XTT assay in studies of *Candida* growth and metabolism. J. Clin. Microbiol. **41:**506–508.
12. **Hua SST, Brandl MT, Hernlem B, Eng JG, Sarreal SBL.** 2011. Fluorescent viability stains to probe the metabolic status of aflatoxigenic fungus in dual culture of *Aspergillus flavus* and *Pichia anomala*. Mycopathologia **171:**133–138.
13. **Gu M, Gan X, Kisteman A, Xu MG.** 2000. Comparison of penetration depth between two-photon excitation and single-photon excitation in imaging through turbid tissue media. Appl. Phys. Lett. **77:**1551–1553.
14. **Theer P, Denk W.** 2006. On the fundamental imaging-depth limit in two-photon microscopy. J. Opt. Soc. Am. A Opt. Image Sci. Vis. **23:**3139–3149.
15. **Gerritsen H, De Grauw C.** 1999. Imaging of optically thick specimen using two-photon excitation microscopy. Microsc. Res. Tech. **47:**206–209.
16. **Masters BR, So PTC, Gratton E.** 1998. Multiphoton excitation microscopy of in vivo human skin: functional and morphological optical biopsy based on three-dimensional imaging, lifetime measurements and fluorescence spectroscopy. Ann. N. Y. Acad. Sci. **838:**58–67.
17. **Zipfel WR, Williams RM, Webb WW.** 2003. Nonlinear magic: multiphoton microscopy in the biosciences. Nat. Biotechnol. **21:**1369–1377.
18. **Huang S, Heikal AA, Webb WW.** 2002. Two-photon fluorescence spectroscopy and microscopy of NAD(P)H and flavoprotein. Biophys. J. **82:**2811–2825.
19. **Laiho LH, Pelet S, Hancewicz TM, Kaplan PD, So PTC.** 2005. Two-photon 3-D mapping of ex vivo human skin endogenous fluorescence species based on fluorescence emission spectra. J. Biomed. Opt. **10:**024016.
20. **Palero JA, de Bruijn HS, van der Ploeg van den Heuvel A, Sterenborg HJCM, Gerritsen HC.** 2007. Spectrally resolved multiphoton imaging of in vivo and excised mouse skin tissues. Biophys. J. **93:**992–1007.
21. **Knaus H, Blab GA, van Veluw GJ, Gerritsen HC, Wösten HAB.** 2013. Label-free fluorescence microscopy in fungi. Fungal Biol. Rev **27:**60–66.
22. **Teuchner K, Ehlert J, Freyer W, Leupold D, Altmeyer P, Stücker M, Hoffmann K.** 2000. Fluorescence studies of melanin by stepwise two-photon femtosecond laser excitation. J. Fluoresc. **10:**275. doi:10.1023/A:1009453228102.
23. **Garini Y, Young IT, McNamara G.** 2006. Spectral imaging: principles and applications. Cytometry A **69:**735–747.
24. **Neher RA, Mitkovski M, Kirchhoff F, Neher E, Theis FJ, Zeug A.** 2009. Blind source separation techniques for the decomposition of multiply labeled fluorescence images. Biophys. J. **96:**3791–3800.
25. **Fereidouni F, Bader AN, Colonna A, Gerritsen HC.** 11 April 2013. Phasor analysis of multiphoton spectral images distinguishes autofluorescence components of in vivo human skin. J. Biophotonics [Epub ahead of print.]. doi:10.1002/jbio.201200244.
26. **Gardecki J, Maroncelli M.** 1998. Set of secondary emission standards for

calibration of the spectral responsivity in emission spectroscopy. Appl. Spectrosc. **52:**1179–1189.
27. **Palero JA, de Bruijn HS, van der Ploeg-van den Heuvel A, Sterenborg HJCM, Gerritsen HC.** 2006. In vivo nonlinear spectral imaging in mouse skin. Opt. Express **14:**4395–4402.
28. **Fereidouni F, Bader AN, Gerritsen HC.** 2012. Spectral phasor analysis allows rapid and reliable unmixing of fluorescence microscopy spectral images. Opt. Express **20:**12729–12741.
29. **Doores S, Kramer M, Beelman R.** 1987. Evaluation and bacterial populations associated with fresh mushrooms (*Agaricus bisporus*). Dev. Crop Sci. **10:**283–294.
30. **Egbebi A, Fakoya S.** 2011. Comparative studies on close button and open cup mushrooms of *Agaricus bisporus*. Int. J. Trop. Med. Public Health **1:**11–17.
31. **Chance B, Schoener B, Oshino R, Itshak F, Nakase Y.** 1979. Oxidation-reduction ratio studies of mitochondria in freeze-trapped samples. NADH and flavoprotein fluorescence signals. J. Biol. Chem. **254:**4764–4771.
32. **Burton K, Love M, Smith J.** 1993. Biochemical changes associated with mushroom quality in *Agaricus* spp. Enzyme Microb. Technol. **15:**736–741.
33. **Soler-Rivas C, Arpin N, Olivier J, Wichers H.** 2000. Discoloration and tyrosinase activity in *Agaricus bisporus* fruit bodies infected with various pathogens. Mycol. Res. **104:**351–356.
34. **Soler-Rivas C, Jolivet S, Arpin N, Olivier JM, Wichers HJ.** 1999. Biochemical and physiological aspects of brown blotch disease of *Agaricus bisporus*. FEMS Microbiol. Rev. **23:**591–614.
35. **Jolivet S, Arpin N, Wichers HJ, Pellon G.** 1998. *Agaricus bisporus* browning: a review. Mycol. Res. **102:**1459–1483.
36. **Butler M, Day A.** 1998. Fungal melanins: a review. Can. J. Microbiol. **44:**1115–1136.
37. **Eisenman HC, Casadevall A.** 2012. Synthesis and assembly of fungal melanin. Appl. Microbiol. Biotechnol. **93:**931–940.
38. **De Groot PW, Schaap PJ, Sonnenberg AS, Visser J, Van Griensven LJ.** 1996. The *Agaricus bisporus hypA* gene encodes a hydrophobin and specifically accumulates in peel tissue of mushroom caps during fruit body development. J. Mol. Biol. **257:**1008–1018.
39. **Lugones LG, Bosscher JS, Scholtmeyer K, de Vries OM, Wessels JGH.** 1996. An abundant hydrophobin (ABH1) forms hydrophobic rodlet layers in *Agaricus bisporus* fruiting bodies. Microbiology **142:**1321–1329.
40. **Schaap PJ, Müller Y, Sonnenberg AS, van Griensven LJ, Visser J.** 1997. The *Agaricus bisporus pruA* gene encodes a cytosolic Δ^1-pyrroline-5-carboxylate dehydrogenase which is expressed in fruit bodies but not in gill tissue. Appl. Environ. Microbiol. **63:**57–62.
41. **De Groot PW, Roeven RT, Van Griensven LJ, Visser J, Schaap PJ.** 1999. Different temporal and spatial expression of two hydrophobin-encoding genes of the edible mushroom *Agaricus bisporus*. Microbiology **145:**1105–1113.
42. **Heneghan MN, Porta C, Zhang C, Burton KS, Challen MP, Bailey AM, Foster GD.** 2009. Characterization of serine proteinase expression in *Agaricus bisporus* and *Coprinopsis cinerea* by using green fluorescent protein and the *A. bisporus* SPR1 promoter. Appl. Environ. Microbiol. **75:**792–801.
43. **Sreenivasaprasad S, Eastwood DC, Browning N, Lewis SM, Burton KS.** 2006. Differential expression of a putative riboflavin-aldehyde-forming enzyme (raf) gene during development and post-harvest storage and in different tissue of the sporophore in *Agaricus bisporus*. Appl. Microbiol. Biotechnol. **70:**470–476.
44. **Kingsnorth CS, Eastwood DC, Burton KS.** 2001. Cloning and postharvest expression of serine proteinase transcripts in the cultivated mushroom *Agaricus bisporus*. Fungal Genet. Biol. **32:**135–144.
45. **Vinck A, Terlou M, Pestman WR, Martens EP, Ram AF, Van Den Hondel CA, Wösten HAB.** 2005. Hyphal differentiation in the exploring mycelium of *Aspergillus niger*. Mol. Microbiol. **58:**693–699.
46. **Vinck A, de Bekker C, Ossin A, Ohm RA, de Vries RP, Wösten HAB.** 2011. Heterogenic expression of genes encoding secreted proteins at the periphery of *Aspergillus niger* colonies. Environ. Microbiol. **13:**216–225.
47. **van Veluw GJ, Teertstra WR, de Bekker C, Vinck A, van Beek N, Muller WH, Arentshorst M, van der Mei HC, Ram AFJ, Dijksterhuis J, Wösten HAB.** 2013. Heterogeneity in liquid shaken cultures of *Aspergillus niger* inoculated with melanised conidia or conidia of pigmentation mutants. Stud. Mycol. **74:**47–57.
48. **de Bekker C, Bruning O, Jonker MJ, Breit TM, Wösten HAB.** 2011. Single cell transcriptomics of neighboring hyphae of *Aspergillus niger*. Genome Biol. **12:**R71. doi:10.1186/gb-2011-12-8-r71.
49. **Bleichrodt RJ, Veluw GJ, Recter B, Maruyama J, Kitamoto K, Wösten HAB.** 2012. Hyphal heterogeneity in *Aspergillus oryzae* is the result of dynamic closure of septa by Woronin bodies. Mol. Microbiol. **86:**1334–1344.